doi.org/10.26434/chemrxiv.11323016.v1

Relation Between Local Structure, Electric Dipole and Charge Carrier Dynamics in DHICA Melanin, a Model for Biocompatible Semiconductors

Micaela Matta, Alessandro Pezzella, Alessandro Troisi

Submitted date: 05/12/2019 • Posted date: 13/12/2019

Citation information: Matta, Micaela; Pezzella, Alessandro; Troisi, Alessandro (2019): Relation Between Local Structure, Electric Dipole and Charge Carrier Dynamics in DHICA Melanin, a Model for Biocompatible Semiconductors. ChemRxiv. Preprint. https://doi.org/10.26434/chemrxiv.11323016.v1

Eumelanins are a family of natural and synthetic pigments obtained by oxidative polymerization of their natural precursors: 5,6 dihydroxyindole and its 2-carboxy derivative (DHICA). The simultaneous presence of ionic and electronic charge carriers makes these pigments promising materials for applications in bioelectronics. In this computational study we build a structural model of DHICA melanin considering the interplay between its many degrees of freedom, then we examine the electronic structure of representative oligomers. We find that a non-vanishing dipole along the polymer chain sets this system apart from conventional polymer semiconductors, determining its electronic structure, reactivity toward oxidation and localization of the charge carriers. Our work sheds light on previously unnoticed features of DHICA melanin that not only fit well with its radical scavenging and photoprotective properties, but open new perspectives towards understanding and tuning charge transport in this class of materials.

Relation Between Local Structure, Electric Dipole and Charge Carrier Dynamics in DHICA Melanin, a Model for Biocompatible Semiconductors

Micaela Matta[1], Alessandro Pezzella[2,3] and Alessandro Troisi[1]*

[1] University of Liverpool, Department of Chemistry, Crown St., Liverpool L69 7ZD, U.K.

[2] National Interuniversity Consortium of Materials Science and Technology (INSTM), Florence, Italy

[3] Institute for Polymers, Composites and Biomaterials (IPCB), CNR, Via Campi Flegrei 34, I-80078 Pozzuoli, NA, Italy

*micaela.matta@liverpool.ac.uk

Abstract

Eumelanins are a family of natural and synthetic pigments obtained by oxidative polymerization of their natural precursors: 5,6 dihydroxyindole and its 2-carboxy derivative (DHICA). The simultaneous presence of ionic and electronic charge carriers makes these pigments promising materials for applications in bioelectronics. In this computational study we build a structural model of DHICA melanin considering the interplay between its many degrees of freedom, then we examine the electronic structure of representative oligomers. We find that a non-vanishing dipole along the polymer chain sets this system apart from conventional polymer semiconductors, determining its electronic structure, reactivity toward oxidation and localization of the charge carriers. Our work sheds light on previously unnoticed features of DHICA melanin that not only fit well with its radical scavenging and photoprotective properties, but open new perspectives towards understanding and tuning charge transport in this class of materials.

Keywords: 5,6-dihydroxyindole, DHICA, density functional theory, eumelanin, charge transport, bioelectronics, mixed conduction, electric dipole, hydrogen bonds

Melanins are a family of natural pigments ubiquitous in mammals and invertebrates. Amongst them, eumelanin is the dark pigment present not only in human skin and hair, but also in eyes and nigral neurons.[1] Due to its dual protonic and electronic conductivity[2–4] and intrinsic biocompatibility, eumelanin is currently being investigated as an active material in supercapacitors for energy storage[5], organic electrochemical field effect transistors (OECTs) for sensing or diagnostics devices, such as cells/nerves stimulation and signal amplification.[6–11] Natural eumelanin consists of amorphous aggregates obtained by oxidative polymerization of 5,6-dihydroxyindole (DHI) and its 2-carboxylic acid derivative (DHICA), interacting via π-stacking and hydrogen bonding (see **Figure 1a**). DHI exhibits self-coupling at position 2, 4 and 7; in DHICA, only positions 4 and 7 are reactive. The structural ambiguity of natural eumelanin, which contains both DHI and DHICA, is partly due to the range of possible binding motifs between the

two building blocks. The development of synthetic DHICA and DHI melanins[12] has paved the way towards a more systematic understanding of the structural, redox, optical and aggregation-dependent properties of eumelanin. The lower structural disorder and better reproducibility make these polymers ideal candidates for exploring the potential of eumelanin in bioelectronic applications, either alone or as a component in hybrid scaffolds.[13]

However, despite its promising characteristics, eumelanin-based devices are still in their infancy. The lack of consensus regarding the molecular structure of both natural and synthetic eumelanin has prevented the rational optimization of semiconducting interfaces based on this biopigment. Moreover, several controversies regarding key properties of eumelanin are yet to be definitively settled. The relative importance of ionic and electronic charge carriers, the influence of water on conductivity and the activity of radical species are still subject of intense academic debate.[14] Several studies argue that the observed increase in conductivity of eumelanin is hydration dependent, and therefore identify the primary charge carriers as protons.[15] However, other studies point at evidence of both electronic and protonic charge transport,[4] and a more recent work reports the highest conductivity ever recorded in vacuum-annealed (anhydrous) melanin films.[2]

Modeling and simulations are therefore indispensable to tackle these issues and push the boundaries of eumelanin bioelectronics. Previous theoretical investigations have focused on reproducing the photophysical features of eumelanin by studying binding motifs between monomers, and π-stacking of small oligomers.[16–18] Others studies have employed molecular dynamics to reproduce the short range ordered structure of eumelanin amorphous aggregates, focusing on porphyrin-like tetramers.[19] Overall, the vast majority of literature has concentrated mostly on planar oligomers of DHI, while DHICA melanin has only been studied marginally.[20,21] Remarkably, no studies have so far investigated charge transport on either system.

The charge transport mechanism of eumelanin is undoubtedly the area where a theoretical insight is most needed to integrate state of the art experimental observations. If we treat eumelanin as a member of the general class of polymer semiconductors, we can assume electron or hole transport would involve the study of more or less extended charge carrier states which are in turn determined by the local microstructure of the material, its mesoscopic properties, and its relative disorder.[22,23] However, eumelanin differs from the typical semiconducting polymer in several nontrivial ways, which characterize its structural disorder. For instance, the hydroxyl units are responsible for the presence of multiple oxidation states; its hydrogen bonds create a non-vanishing dipole across the polymer chain, and the nonsymmetric nature of its monomers makes the corresponding polymers not regioregular.

In the specific case of DHICA melanin, we have categorized the degrees of freedom that can be sees as the origin of the structural disordered in the polymer:

- ***Tacticity/regiochemistry***. For both DHI and DHICA, position 4 and 7 are not equivalent, giving rise to different binding motifs illustrated in **Figure 1b** and denoted as 4,4′, 7,7′ and 4,7′. Oligomers with different regiochemistry have been isolated[20,24] but the distribution of tacticity in realistic materials and its effect on the electronic structure is not known.
- ***Conformational isomerism (atropoisomerism) and helicity***. The rotation around the C-C′ bonds is hindered, thus different diastereoisomers are possible for the same chemical connectivity, depending on the dihedral angles between indole units. Helicity, defined as the collective orientation of all dihedrals between monomers, not only influences the DHICA polymer shape but could also affect inter-chain interactions and aggregation.

- ***Hydrogen bond network***. Non-bonded interactions, particularly inter- and intra-chain hydrogen bonds and inter-chain π-stacking, might strongly affect the polymer structure. In particular the –OH groups form a 1D chain of H-bond donor/acceptor (see **Figure 1c**) which can, in principle, dictate the local conformation of the polymer.[21]
- ***Oxidation state and redox disorder***. DHICA oligomers tend to oxidize as the polymer grows beyond ~10 repeating units[25], the main oxidized species being the quinone. The distribution of quinone units within the polymer is not completely understood, but it is estimated that one in 20 monomers is oxidized.[26,27] Two main oxidation patterns are possible: distributed and localized (see **Figure 1d**), with the latter being more stable according to prior studies. The presence of oxidized groups gives DHICA melanin its spectroscopic signature, being responsible for the broad absorption in the UV-Vis region. The change in electronic structure upon oxidation is bound to affect the charge transport properties, although this aspect has not been investigated so far.

In this work, we study DHICA oligomers to establish how the many degrees of freedom of this system interact to determine the most stable structure, working our way from the highest interconversion barriers to the lowest: tacticity, atropoisomerism, helicity, hydrogen bond network. Once established the hierarchy of structural degrees of freedom, we turn our attention to oxidized oligomers and the effects of oxidation on the electronic structure of DHICA melanin, concluding with general considerations about the most likely charge transport mechanisms in this material.

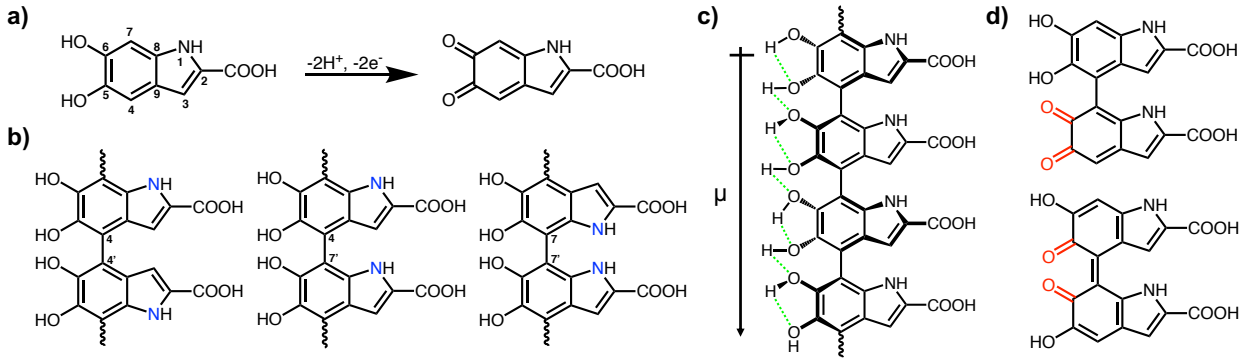

Figure 1. a) Molecular structure and ring numbering of DHICA in the reduced indole (left) form and in the oxidized quinone form (right). **b)** Different tacticity in DHICA melanin originating from 4,4′ (left), 4,7′ (center) and 7,7′ (right) bonds. Rotation around these single bonds is sterically hindered. **c)** Scheme of a DHICA tetramer highlighting the atropoisomerism, the hydrogen bonds network and the direction of the oligomer dipole **d)** Localized (top) and distributed (bottom) oxidation pattern for quinones.

Tacticity and conformational isomerism. As previously reported, all 4,4′, 4,7′ and 7,7′ DHICA dimers have their lowest energy minimum at ~50° (see Supporting Information, Figure S1), characterized by an inter-monomer hydrogen bond. The 4,7′ isomer is the most stable, followed by 4,4′ and 7,7′ (higher in energy by 0.88 and 1.77 kcal/mol, respectively). Regardless of energy differences, all three minima look similar and the curvature of their potential energy surface is almost identical. Remarkably, the three most stable dimers have very similar dipole moments (5.7-5.9 Debye), oriented along the polymer growth axis and largely due to the inter- and intramolecular hydrogen bonds. These findings highlight the limited importance of tacticity in the conformational

landscape of DHICA melanin and, we argue, in determining its charge transport properties. Therefore, for the remainder of this discussion we will focus on 4,7′ regioregular oligomers.

Helicity and hydrogen bond network. We considered two hypotheses regarding the collective orientation of dihedrals in longer oligomers: they can be arranged in a zig-zag fashion, alternating ±50° dihedrals, or in a helix shape, all dihedrals having the same sign, as shown in **Figure 2a**. The zig zag shaped oligomers are only slightly preferred to the helix shaped, by 0.28 (0.87) kcal/mol for tetramers (octamers). As the difference between the two conformations is substantially smaller than typical intramolecular interactions (i.e. hydrogen bonds), we can assume the final helicity (defined as the sequence of dihedrals between monomers) will be likely determined by the local environment, which lies outside the scope of this study.

Both zig-zag and helix oligomers are stabilized by an uninterrupted chain of hydrogen bonds in same direction of the indole dipole, with hydroxyl groups pointing the opposite way with respect to the nitrogen (see **Figure 2a**). The consequence of the hydrogen bond directionality is that the individual dipoles of each monomer (2.9 Debye) are summed to give a strong, permanent dipole in both helix and zig-zag conformations. (**Figure 2b**). The energy penalty to reverse the direction of all hydrogen bonds is 2.97 (3.02) kcal/mol for a zig-zag (helix) tetramer. We also investigated the penalty for the disruption of the hydrogen bond and dipole continuity by flipping half of the C-C-O-H dihedrals in the opposite direction for tetramers. The energy penalty was found to be 10.3 (9.96) kcal/mol for the zig-zag (helix) conformation, and rather insensitive to the chain length (see Figure S1 and Table S2). Interestingly, the energy difference between the zig-zag and helix conformations is reduced to just 0.06 kcal/mol once the chain of hydrogen bonds is disrupted (Figure S2 and Table S2). These observations denote that hydrogen bonds and torsional energies are additive.

In summary, tacticity and helicity are predicted to have little effect on the electronic structure of DHICA melanin, the most stable arrangement of dihedrals maximises the internal dipole by forming an uninterrupted chain of hydrogen bonds. However, we must point out that the energy cost to disrupt the dipoles could be easily circumvented via the formation of intermolecular hydrogen bonds, a possibility we are not explicitly considering in this work.

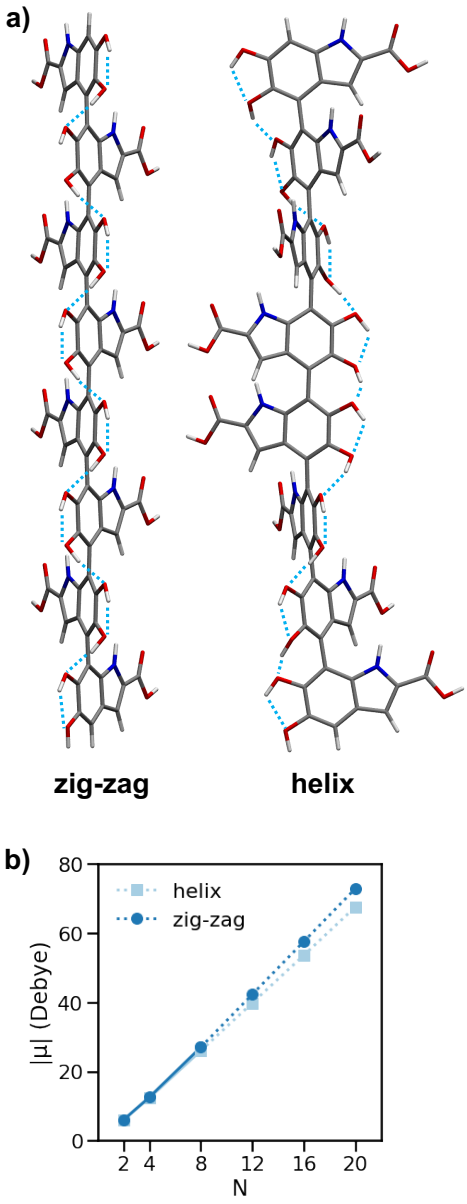

Figure 2. a) Optimized geometries of octamers in the zig-zag and helix conformations, with dotted lines highlighting the chain of hydrogen bonds. **b)** Absolute magnitude of the dipole as a function of oligomer length N for a series of zig-zag and helix oligomers. Points connected by solid lines indicate fully optimized geometries at wB97XD/6-31G* level, dashed lines identify wB97XD/6-31G* single point calculations on longer oligomers obtained by rigid translation of shorter segments.

Oxidation to quinone. Once established the hierarchy of interactions dictating the conformational space of DHICA oligomers, we studied the corresponding quinones, under the generally accepted assumption that polymerization (at least in its initial phase) happens prior to oxidation.[25] Helix and zig-zag tetramers were oxidized to quinones; all possible oxidation patterns, both distributed and localized, were explored (see Supporting Information, Figure S3). As expected, localized quinones are energetically preferred by 1.4 (0.9) kcal/mol for zig-zag (helix) tetramers. Interestingly, there is a strong effect of the internal dipole, which favors oxidation on the terminal (negative) monomer,

followed by the second to last (0.3 kcal/mol higher in energy), and makes the opposite (positive) end harder to oxidize (3.75 and 4.53 kcal/mol more endothermic for zig-zag and helix tetramers respectively). As seen for the corresponding indoles, the energy difference between the 2 most stable quinones in either zig-zag or helix conformation remains rather small at 0.43 kcal/mol. Since chain helicity does not seem to affect the relative stability of quinone isomers, we will only focus on longer oligomers in the zig-zag conformation.

We then studied the interaction between quinones by oxidizing two monomers on the same zig-zag octamer. Using the most stable singly oxidized species as references, we calculated the energy penalty for the products of a second oxidation at different positions with respect to the first quinone (see Supporting Information, Figure S4 and S5a). The results show that a second oxidation is less energetically favored near an already oxidized indole suggesting that the oxidation sites have a tendency to be segregated. In general, we would expect oxidation to occur at a position that minimizes the repulsion with other quinones and maximizes the distance from the positive end of the dipole. Quinone units introduce a discontinuity in the hydrogen bond network, so DHICA melanin can be visualized as made of long segments with unidirectional hydrogen bonds interrupted by oxidized units.

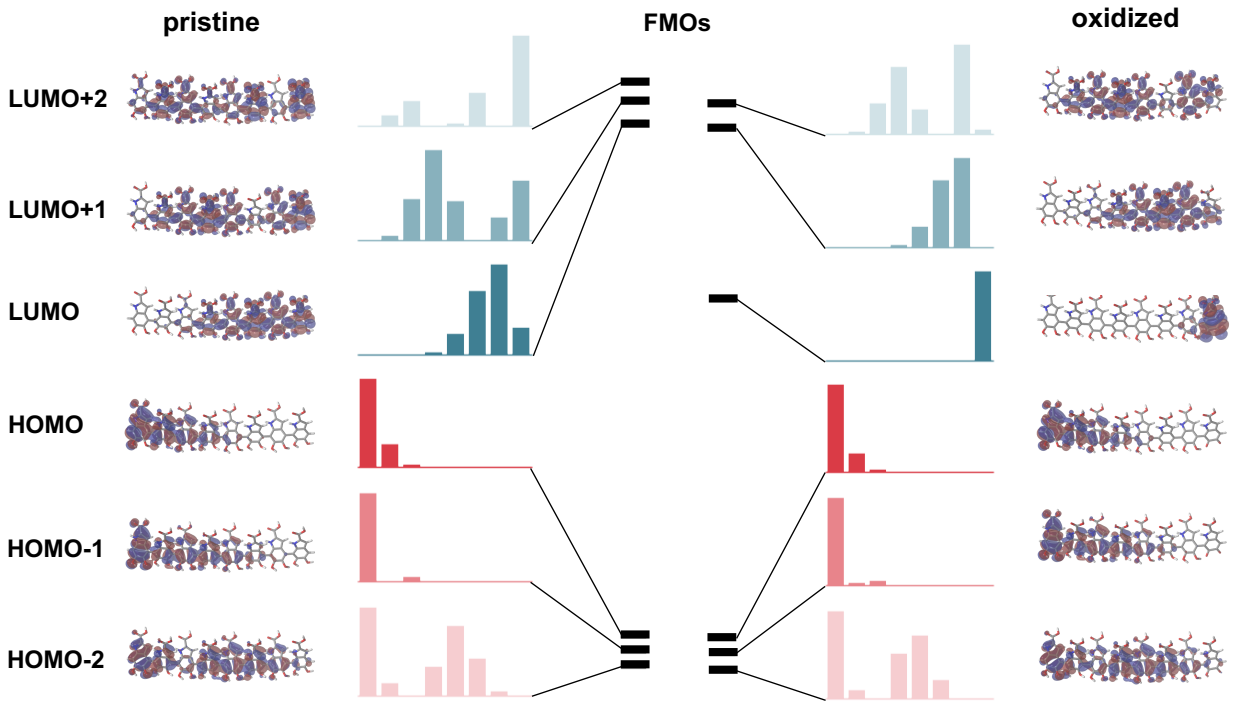

Figure 3. Frontier molecular orbitals (HOMO-2 to LUMO+2), squared fragment orbital population coefficients on each monomer obtained from the Mulliken population analysis and energy diagram of the reduced (left) and oxidized (right) octamers.

Energy landscape and transport mechanism of oxidized oligomers. We analyzed the changes in the electronic energy states of oxidized oligomers with respect to their reduced analogues, in particular the shape and localization of frontier molecular orbitals (FMOs). In both species, the strong permanent dipole affects the shape of the frontier orbitals: while the HOMO is localized

towards the negatively charged side of the oligomer, the situation is reversed for the LUMO (see **Figure 3**, left side). This striking effect, unseen in canonic semiconducting polymers, does not stem from the nature of the π-conjugated system but rather from polar functional groups not involved in conjugation. Oxidation is accompanied by the appearance of a low lying LUMO localized on the quinone unit, leaving the other FMOs unperturbed (see the right-hand side of **Figure 3**). Regardless of the oxidation position, to each quinone corresponds a localized state adding to the lowest energy band in the polymer (Supporting Information, Figure S4b).

The electronic properties of representative DHICA oligomers allow us to formulate predictions on the charge carrier behavior in DHICA melanin. As far as holes are concerned, the internal dipole of the polymer affects the shape and localization of the HOMO, and constitutes a new type of long range, correlated disorder contributing to the localization of holes. As seen in Figure S2, the position of the HOMO along the DHICA oligomer is strongly affected by the dipole orientation; this would seem to favor the localization of holes and electrons in different segments, at least in small oligomers with only one oxidation defect. However, a more representative model oligomer would be a longer segment where a series of indole units are delimited by a quinone on either end (see **Figure 4**). In this model system, regardless of the local dipole orientation, the hole is found to overlap with one of the two quinone-centered monomers. The energy to escape this local trap, either towards another localized state[28] or to a more delocalized state, is given by the reorganization energy, λ_+=~0.8 eV (see Supporting Information, Table S3). The density of these traps is comparable to the density of oxidized units and typically similar or larger to the carrier density achievable in transistor devices, we expect these localized states to determine the carrier mobility in most conditions. This is a highly unusual scenario for polymer semiconductors, where conformational disorder is the main factor affecting charge transport.[29–31]

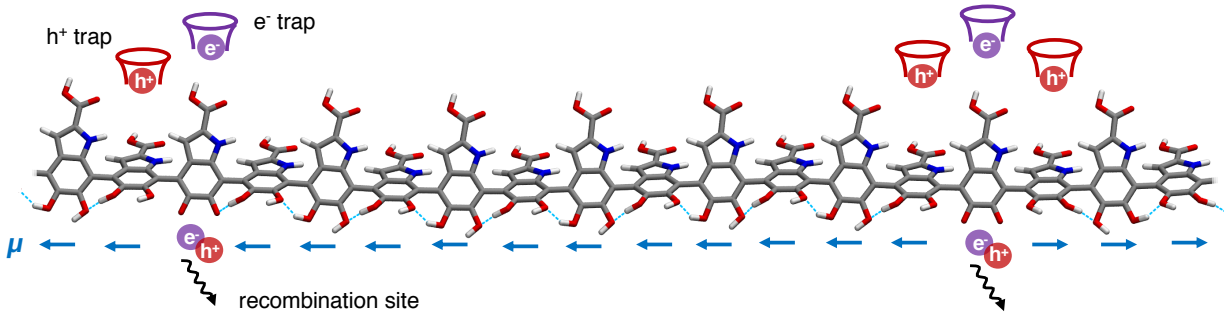

Figure 4. Scheme of a DHICA melanin segment showing typical recombination and trapping sites for holes and electrons. The monomer dipoles (blue arrows) follow the direction of the hydrogen bonds.

Conversely, electrons are expected to be localized on isolated oxidized monomers, the electron affinity of an oxidized oligomer being 2.3 eV higher than that of its polyindole analogue (see Table S3). Given the low density of quinones across the polymer chain, as well as the significant energy difference between these trap states and the higher, more delocalized unoccupied states, we do not anticipate electron transport to be relevant in DHICA melanin. Interestingly, the ambiguity surrounding the exact nature of the spatially confined and roughly homogeneous free radical species in DHICA melanin,[32] characterized by a narrow EPR signal, seems to agree with our findings regarding the spatial localization of both holes and electrons.

As for the fate of electron-hole pairs, the significant spatial overlap between localized holes and electrons is expected to lead to efficient charge recombination. This would be the case when electron-hole pairs are photochemically generated, thus concurring to the efficient non-radiative energy dissipation mechanism crucial for the pigment's photoprotective activity.[33]

Conclusion

In this work, we uncovered a number of features that set DHICA melanin aside from other biopolymers as well as common organic semiconductors. We set out to study the regiochemistry and conformational freedom of DHICA melanin, only to discover their marginal role in determining both the charge carrier and orbital localization. The electronic structure of DHICA melanin is surprisingly and substantially affected by its strong dipole moment, which localizes frontier orbitals on small molecular segments and impacts the polymer charge transport mechanism. The formation of one-dimensional chains of hydrogen bonds is DHICA melanin's defining structural feature, and their orientation directly affects the dipole magnitude. The disruption of the hydrogen bond network is then anticipated to be one of the main sources of electronic disorder in the bulk. Oxidation is instead shown to create extremely localized virtual orbitals, building up a separate band in the density of states of the bulk polymer. Hole transport in DHICA melanin is likely to happen via hopping, however limited by the presence of deep trap states. Future studies aimed at obtaining a full picture of DHICA melanin will take into account the effect of stabilizing inter-chain interactions, chain flexibility and a higher dielectric environment that would concur to reduce the hydrogen bond orientational order.

The wider impact of our findings is related to the possible role of eumelanin as a biocompatible semiconductor. To this end, we can anticipate chemical modification and functionalization to play a main role in tuning the transport properties in this class of materials, where electrostatic interactions are more important role than non-polar, Van der Waals forces.

Computational Methods

Geometry optimizations were performed with Gaussian16[34] at the wB97XD/6-31G* level except where otherwise stated. The Mulliken population analysis was performed using the cclib[35] package.

Supporting Information

Supplementary materials, including details of conformational searches and electronic structure calculations, are available as a pdf file.

Acknowledgements

M. M. acknowledges the financial support of the Royal Society in the form of a Newton International Fellowship.

Author contributions

M.M. realized the study and wrote the paper. M. M., A.T. and A.P. designed the study.

Notes

The authors declare no competing financial interests.

References

(1) d'Ischia, M.; Wakamatsu, K.; Cicoira, F.; Di Mauro, E.; Garcia-Borron, J. C.; Commo, S.; Galván, I.; Ghanem, G.; Kenzo, K.; Meredith, P.; et al. Melanins and Melanogenesis: From Pigment Cells to Human Health and Technological Applications. *Pigment Cell Melanoma Res.* **2015**, *28* (5), 520–544. https://doi.org/10.1111/pcmr.12393.

(2) Migliaccio, L.; Manini, P.; Altamura, D.; Giannini, C.; Tassini, P.; Maglione, M. G.; Minarini, C.; Pezzella, A. Evidence of Unprecedented High Electronic Conductivity in Mammalian Pigment Based Eumelanin Thin Films After Thermal Annealing in Vacuum. *Front. Chem.* **2019**, *7* (March), 1–8. https://doi.org/10.3389/fchem.2019.00162.

(3) Wünsche, J.; Cicoira, F.; Graeff, C. F. O.; Santato, C. Eumelanin Thin Films: Solution-Processing, Growth, and Charge Transport Properties. *J. Mater. Chem. B* **2013**, *1* (31), 3836. https://doi.org/10.1039/c3tb20630k.

(4) Wünsche, J.; Deng, Y.; Kumar, P.; Di Mauro, E.; Josberger, E.; Sayago, J.; Pezzella, A.; Soavi, F.; Cicoira, F.; Rolandi, M.; et al. Protonic and Electronic Transport in Hydrated Thin Films of the Pigment Eumelanin. *Chem. Mater.* **2015**, *27* (2), 436–442. https://doi.org/10.1021/cm502939r.

(5) Kumar, P.; Di Mauro, E.; Zhang, S.; Pezzella, A.; Soavi, F.; Santato, C.; Cicoira, F. Melanin-Based Flexible Supercapacitors. *J. Mater. Chem. C* **2016**, *4* (40), 9516–9525. https://doi.org/10.1039/C6TC03739A.

(6) Piacenti Da Silva, M.; Fernandes, J. C.; De Figueiredo, N. B.; Congiu, M.; Mulato, M.; De Oliveira Graeff, C. F. Melanin as an Active Layer in Biosensors. *AIP Adv.* **2014**, *4* (3).

(7) Bonadies, I.; Cimino, F.; Carfagna, C.; Pezzella, A. Eumelanin 3D Architectures: Electrospun PLA Fiber Templating for Mammalian Pigment Microtube Fabrication. *Biomacromolecules* **2015**, *16* (5), 1667–1670. https://doi.org/10.1021/acs.biomac.5b00239.

(8) Pezzella, A.; Barra, M.; Musto, A.; Navarra, A.; Alfè, M.; Manini, P.; Parisi, S.; Cassinese, A.; Criscuolo, V.; D'Ischia, M. Stem Cell-Compatible Eumelanin Biointerface Fabricated by Chemically Controlled Solid State Polymerization. *Mater. Horizons* **2015**, *2* (2), 212–220. https://doi.org/10.1039/c4mh00097h.

(9) Rivnay, J.; Inal, S.; Salleo, A.; Owens, R. M.; Berggren, M.; Malliaras, G. G. Organic Electrochemical Transistors. *Nat. Rev. Mater.* **2018**, *3* (2), 17086. https://doi.org/10.1038/natrevmats.2017.86.

(10) Paulsen, B. D.; Tybrandt, K.; Stavrinidou, E.; Rivnay, J. Organic Mixed Ionic–Electronic

Conductors. *Nat. Mater.* **2019**. https://doi.org/10.1038/s41563-019-0435-z.

(11) Inal, S.; Malliaras, G. G.; Rivnay, J. Benchmarking Organic Mixed Conductors for Transistors. *Nat. Commun.* **2017**, *8* (1), 1767. https://doi.org/10.1038/s41467-017-01812-w.

(12) D'Ischia, M.; Wakamatsu, K.; Napolitano, A.; Briganti, S.; Garcia-Borron, J. C.; Kovacs, D.; Meredith, P.; Pezzella, A.; Picardo, M.; Sarna, T.; et al. Melanins and Melanogenesis: Methods, Standards, Protocols. *Pigment Cell and Melanoma Research*. 2013. https://doi.org/10.1111/pcmr.12121.

(13) Di Capua, R.; Gargiulo, V.; Alfè, M.; De Luca, G. M.; Skála, T.; Mali, G.; Pezzella, A. Eumelanin Graphene-Like Integration: The Impact on Physical Properties and Electrical Conductivity. *Front. Chem.* **2019**, *7* (March), 1–12. https://doi.org/10.3389/fchem.2019.00121.

(14) Rienecker, S. B.; Mostert, A. B.; Schenk, G.; Hanson, G. R.; Meredith, P. Heavy Water as a Probe of the Free Radical Nature and Electrical Conductivity of Melanin. *J. Phys. Chem. B* **2015**, *119* (48), 14994–15000. https://doi.org/10.1021/acs.jpcb.5b08970.

(15) Sheliakina, M.; Mostert, A. B.; Meredith, P. An All-Solid-State Biocompatible Ion-to-Electron Transducer for Bioelectronics. *Mater. Horizons* **2018**, *5* (2), 256–263. https://doi.org/10.1039/C7MH00831G.

(16) Prampolini, G.; Cacelli, I.; Ferretti, A. Intermolecular Interactions in Eumelanins: A Computational Bottom-up Approach. I. Small Building Blocks. *RSC Adv.* **2015**, *5* (48), 38513–38526. https://doi.org/10.1039/c5ra03773e.

(17) Chen, C. T.; Buehler, M. J. Polydopamine and Eumelanin Models in Various Oxidation States. *Phys. Chem. Chem. Phys.* **2018**, *20* (44), 28135–28143. https://doi.org/10.1039/c8cp05037f.

(18) Chen, C. T.; Martin-Martinez, F. J.; Jung, G. S.; Buehler, M. J. Polydopamine and Eumelanin Molecular Structures Investigated with Ab Initio Calculations. *Chem. Sci.* **2017**, *8* (2), 1631–1641. https://doi.org/10.1039/C6SC04692D.

(19) Chen, C. T.; Chuang, C.; Cao, J.; Ball, V.; Ruch, D.; Buehler, M. J. Excitonic Effects from Geometric Order and Disorder Explain Broadband Optical Absorption in Eumelanin. *Nat. Commun.* **2014**, *5* (May), 1–10. https://doi.org/10.1038/ncomms4859.

(20) Pezzella, A.; Vogna, D.; Prota, G. Synthesis of Optically Active Tetrameric Melanin Intermediates by Oxidation of the Melanogenic Precursor 5,6-Dihydroxyindole-2-Carboxylic Acid under Biomimetic Conditions. *Tetrahedron: Asymmetry* **2003**, *14* (9), 1133–1140. https://doi.org/10.1016/S0957-4166(03)00156-3.

(21) Pezzella, A.; Panzella, L.; Crescenzi, O.; Napolitano, A.; Navaratnam, S.; Edge, R.; Land, E. J.; Barone, V.; D'Ischia, M. Lack of Visible Chromophore Development in the Pulse Radiolysis Oxidation of 5,6-Dihydroxyindole-2-Carboxylic Acid Oligomers: DFT Investigation and Implications for Eumelanin Absorption Properties. *J. Org. Chem.* **2009**, *74* (10), 3727–3734. https://doi.org/10.1021/jo900250v.

(22) Noriega, R.; Rivnay, J.; Vandewal, K.; Koch, F. P. V; Stingelin, N.; Smith, P.; Toney, M. F.; Salleo, A. A General Relationship between Disorder, Aggregation and Charge

Transport in Conjugated Polymers. *Nat. Mater.* **2013**, *12* (11), 1038–1044. https://doi.org/10.1038/nmat3722.

(23) Fornari, R. P.; Blom, P. W. M.; Troisi, A. How Many Parameters Actually Affect the Mobility of Conjugated Polymers? *Phys. Rev. Lett.* **2017**, *118* (8), 086601. https://doi.org/10.1103/PhysRevLett.118.086601.

(24) Pezzella, A.; Vogna, D.; Prota, G. Atropoisomeric Melanin Intermediates by Oxidation of the Melanogenic Precursor 5,6-Dihydroxyindole-2-Carboxylic Acid under Biomimetic Conditions. *Tetrahedron* **2002**, *58* (19), 3681–3687. https://doi.org/10.1016/S0040-4020(02)00335-6.

(25) Pezzella, A.; Napolitano, A.; D'Ischia, M.; Prota, G.; Seraglia, R.; Traldi, P. Identification of Partially Degraded Oligomers of 5,6-Dihydroxyindole-2-Carboxylic Acid in Sepia Melanin by Matrix-Assisted Laser Desorption/Ionization Mass Spectrometry. *Rapid Commun. Mass Spectrom.* **1997**. https://doi.org/10.1002/(SICI)1097-0231(19970228)11:4<368::AID-RCM859>3.0.CO;2-E.

(26) Pezzella, A.; Iadonisi, A.; Valerio, S.; Panzella, L.; Napolitano, A.; Adinolfi, M.; D'Ischia, M. Disentangling Eumelanin "Black Chromophore": Visible Absorption Changes as Signatures of Oxidation State- and Aggregation-Dependent Dynamic Interactions in a Model Water-Soluble 5,6-Dihydroxyindole Polymer. *J. Am. Chem. Soc.* **2009**. https://doi.org/10.1021/ja905162s.

(27) Pezzella, A.; Panzella, L.; Crescenzi, O.; Napolitano, A.; Navaratman, S.; Edge, R.; Land, E. J.; Barone, V.; D'Ischia, M. Short-Lived Quinonoid Species from 5,6-Dihydroxyindole Dimers En Route to Eumelanin Polymers: Integrated Chemical, Pulse Radiolytic, and Quantum Mechanical Investigation. *J. Am. Chem. Soc.* **2006**. https://doi.org/10.1021/ja0650246.

(28) Zhang, Y.; Liu, C.; Balaeff, A.; Skourtis, S. S.; Beratan, D. N. Biological Charge Transfer via Flickering Resonance. *Proc. Natl. Acad. Sci. U. S. A.* **2014**. https://doi.org/10.1073/pnas.1316519111.

(29) Jackson, N. E.; Kohlstedt, K. L.; Savoie, B. M.; Olvera de la Cruz, M.; Schatz, G. C.; Chen, L. X.; Ratner, M. A. Conformational Order in Aggregates of Conjugated Polymers. *J. Am. Chem. Soc.* **2015**, *137* (19), 6254–6262. https://doi.org/10.1021/jacs.5b00493.

(30) Wang, S.; Fazzi, D.; Puttisong, Y.; Jafari, M. J.; Chen, Z.; Ederth, T.; Andreasen, J. W.; Chen, W. M.; Facchetti, A.; Fabiano, S. Effect of Backbone Regiochemistry on Conductivity, Charge Density, and Polaron Structure of n-Doped Donor-Acceptor Polymers. *Chem. Mater.* **2019**. https://doi.org/10.1021/acs.chemmater.9b00558.

(31) Qin, T.; Troisi, A. Relation between Structure and Electronic Properties of Amorphous MEH-PPV Polymers. *J. Am. Chem. Soc.* **2013**. https://doi.org/10.1021/ja404385y.

(32) Panzella, L.; Gentile, G.; D'Errico, G.; Della Vecchia, N. F.; Errico, M. E.; Napolitano, A.; Carfagna, C.; D'Ischia, M. Atypical Structural and π-Electron Features of a Melanin Polymer That Lead to Superior Free-Radical-Scavenging Properties. *Angew. Chemie - Int. Ed.* **2013**, *52* (48), 12684–12687. https://doi.org/10.1002/anie.201305747.

(33) Micillo, R.; Panzella, L.; Koike, K.; Monfrecola, G.; Napolitano, A.; D'Ischia, M. "Fifty Shades" of Black and Red or How Carboxyl Groups Fine Tune Eumelanin and

Pheomelanin Properties. *International Journal of Molecular Sciences*. MDPI AG May 17, 2016, p 746. https://doi.org/10.3390/ijms17050746.

(34) Frisch, M. J.; Trucks, G. W.; Schlegel, H. B.; Scuseria, G. E.; Robb, M. A.; Cheeseman, J. R.; Scalmani, G.; Barone, V.; Mennucci, B.; Petersson, G. A.; et al. Gaussian16 (Revision C.01), Gaussian Inc. Wallingford CT. *Gaussian16 (Revision C.01)*. 2016.

(35) O'Boyle, N. M.; Tenderholt, A. L.; Langner, K. M. Cclib: A Library for Package-Independent Computational Chemistry Algorithms. *J. Comput. Chem.* **2008**. https://doi.org/10.1002/jcc.20823.

Supporting Information File

Relation between local structure and nature of charge carriers in DHICA melanin, a model system for mixed conduction

Micaela Matta[1], Alessandro Pezzella[2,3] and Alessandro Troisi[1]*

[1] University of Liverpool, Department of Chemistry, Crown st., Liverpool L69 7ZD
[2] National Interuniversity Consortium of Materials Science and Technology (INSTM), Florence, Italy
[3] Institute for Polymers, Composites and Biomaterials (IPCB), CNR, Via Campi Flegrei 34, I-80078 Pozzuoli, NA, Italy

*micaela.matta@liverpool.ac.uk

1. Potential energy scan of DHICA dimers

The potential energy scan around the C-C-C'-C' dihedral is shown in **Figure S1**. The shape of the PES around the lowest energy minimum of DHICA dimers is dictated by the formation and breaking of an inter-monomer hydrogen bond. The resulting torsional barrier is between 4.2 and 4.7 kcal/mol. The shallow minimum at ~125 degrees appears slightly different for all three species, with the 7,7' one being slightly more pronounced. It should be noted that, due to the shallow barrier for interconversion back to the global minimum, we don't expect the population of the 125 degrees minimum to be significant.
Performing the same torsional scan after reorienting the hydroxyl groups to prevent the formation of the hydrogen bond yields a rather different potential energy surface. For all three dimers, the most stable conformer lies now at ~125°, while the barrier between the two minima is significantly lowered. As observed in the previous torsional scan, there are slight differences in the depth and shape of the ~125° minima. Notably, the whole potential energy curve appears shifted downwards in the case of **D44** and upwards for **D47**.

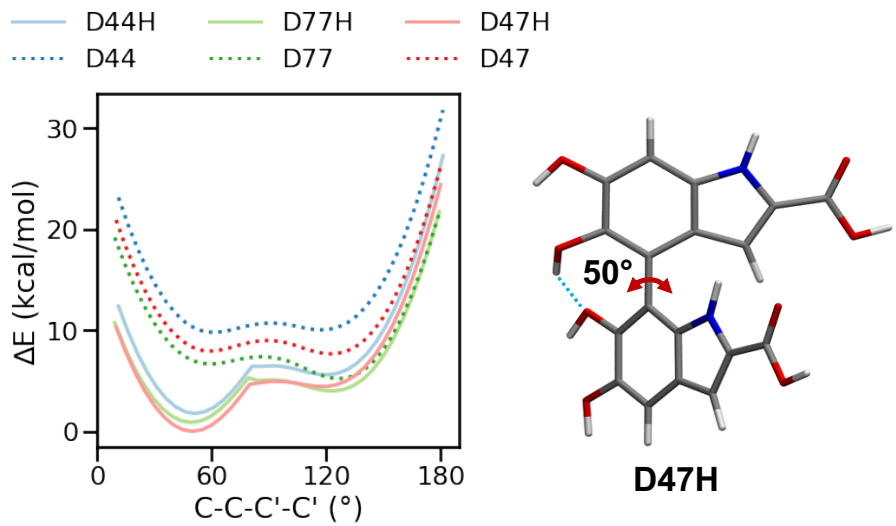

Figure S1. Potential energy scan of the C-C-C'-C' dihedral at the wB97XD/6-31G* level for DHICA dimers in the presence and absence of an intermonomer hydrogen bond. The relative energies are normalized to the absolute lowest minimum, **D47H** (right panel).

Table S1. Optimized parameters of the global minimum of 4,7'-DHICA dimer obtained with different functionals.

Functional	**C-C-C'-C' (º)**	**C-C' (º)**	**O-H' (Å)**
B3LYP	49.87	1.484	1.796
PBE0	48.96	1.477	1.772
M06-2X	49.17	1.479	1.809
wB97XD	49.88	1.481	1.813

2. Dipole analysis and relative energies of DHICA oligomers

The effect of the hydrogen bond orientation on the dipole moment and relative stability of DHICA oligomers was investigated using tetramers and octamers. Results in **Figure S2** and **Table S2** show how to an inversion in the hydrogen bond direction corresponds an inversion in the dipole moment and in the HOMO localization.

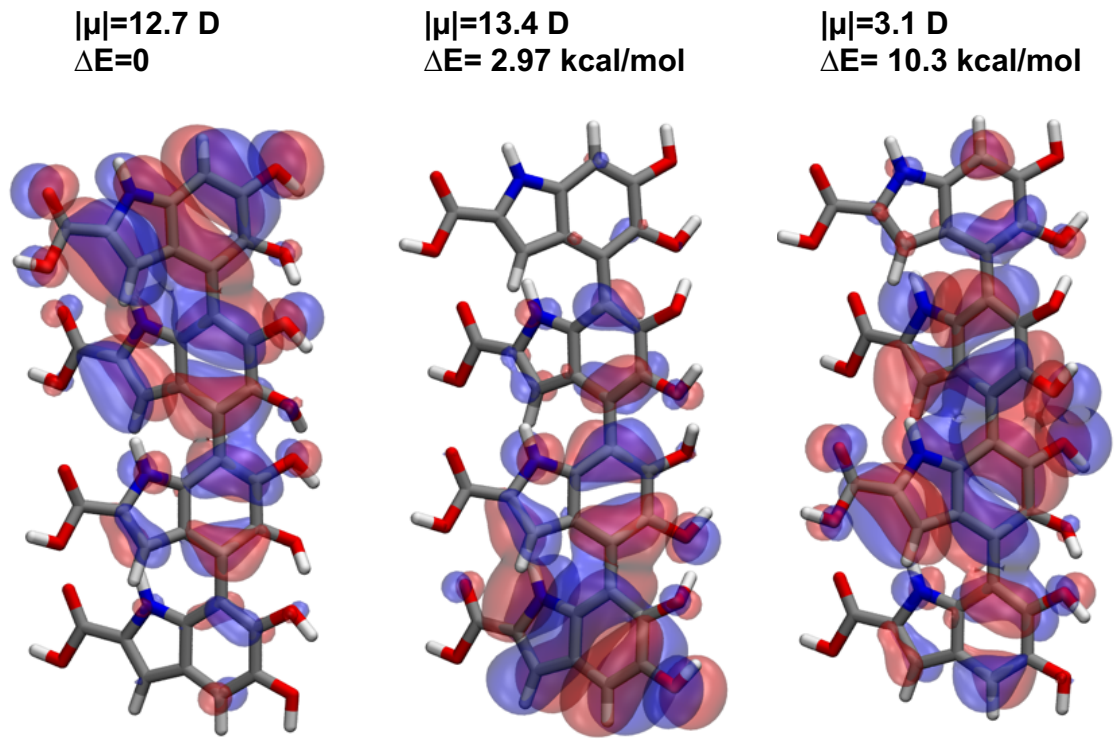

Figure S2. Dipole moments, relative energies and HOMO orbitals of DHICA tetramers optimized with hydrogen bonds pointing downward in the most stable conformation (left), upwards (center), and half upwards and half downwards (right).

Table S2. Dipole moments and relative energies of zig-zag tetramers and octamers as a function of the hydrogen bonds (dipole) direction, obtained from wB97XD/6-31G* optimized geometries. The arrows refer to the hydrogen bond orientation.

Structure	$\|\mu\|$ (Debye)	E_{rel} (kcal/mol)
Tetramer >>	12.7	0
Tetramer <<	13.4	2.97
Tetramer < >	3.1	10.28
Octamer >>	26.68	0
Octamer <<	31.08	3.92
Octamer < >	2.84	12.23

3. Oxidation of DHICA oligomers

Both zig-zag and helix tetramers were oxidized to the corresponding quinones. All localized and distributed quinones were generated. The remaining hydroxyl groups were also rotated so as to maximize the number of hydrogen bonds. All relative energies are reported in **Figure S3**.

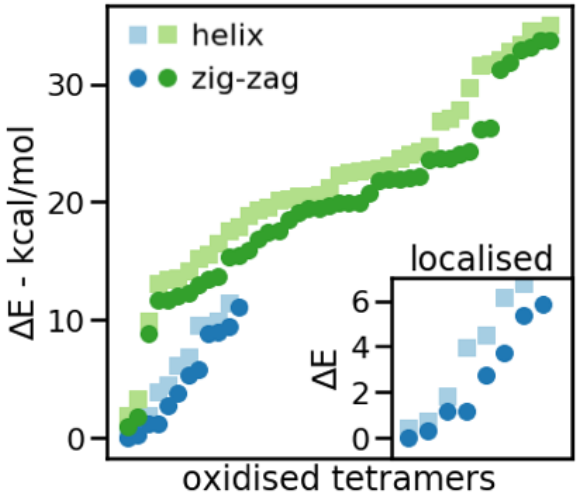

Figure S3. Relative energies of oxidized tetramers ordered from the lowest to the highest, divided in localized (dark/light blue) and distributed (dark/light green). The inset shows the lowest energy localized tetramers. Geometries were optimized at the B3LYP/6-31G* level.

After establishing the most stable oxidized tetramers, the corresponding lowest energy zig-zag octamers $\mathbf{Q_7}$ and $\mathbf{Q_8}$ were optimized at B3LYP/6-31G* level and single-point calculations were performed using the wB97XD/6-31G* level of theory. The energetic penalty for a second oxidation starting from both $\mathbf{Q_7}$ and $\mathbf{Q_8}$ is defined as:

$$\Delta\Delta E_{ox}^{n} = E_{QQ}^{xn} - E_{Q}^{n} - E_{Q}^{x} + E_{I}$$

where E_{QQ}^{xn} is the energy of a doubly oxidized octamer, E_{Q}^{n} and $E_{Q}^{x=7,8}$ those of mono-oxidized octamers $\mathbf{Q_7}$ and $\mathbf{Q_8}$, and E_I is the poly-indole octamer.
The energy diagram for both species is shown in **Figure S5a**. Interestingly, the energy penalty to have a second quinone on the same octamer chain becomes comparable to k_bT if the two oxidation sites are 3-5 monomers apart.

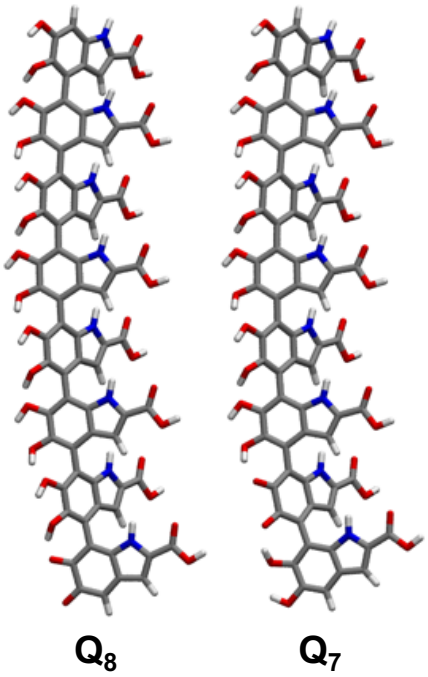

Figure S4. Optimized geometries of the most stable oxidized octamers $\mathbf{Q_8}$ and $\mathbf{Q_7}$ obtained at the wB97XD/6-31G* level.

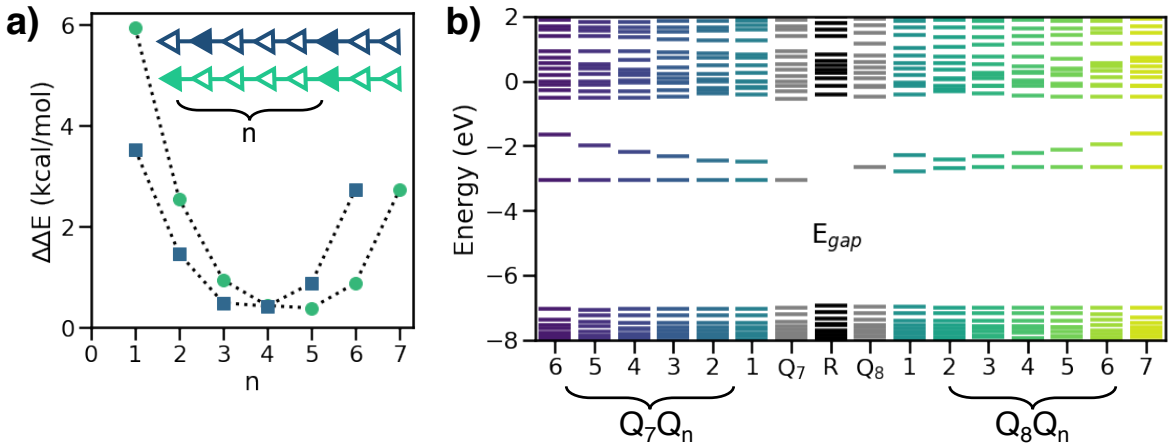

Figure S5. **a)** Calculated energy difference for the second oxidation, $\Delta\Delta E_{ox}^{x}$ for DHICA octamers $\mathbf{Q_7Q_n}$ and $\mathbf{Q_8Q_n}$, with two oxidized monomers, as a function of **n**, the distance between the quinones. **b)** Energy level diagrams for pristine and oxidized DHICA octamers.

4. Reorganization energies, ionization potentials and electron affinities

Ionisation potentials, electron affinities and internal reorganization energies of DHICA octamers were calculated using the wB97XD/6-31G* electronic energies. Reorganization energies were calculated according to the four point method by Nielsen et al. (J. Phys. Chem. B 2008, 112, 35, 11079-11086).
The dependency of the ionization potential on the polymer length was verified by optimizing oligomers of different length (see **Figure S6**). The results show that octamers provide a reasonably good estimate for the ionization potential of DHICA melanin.
Table S3 below summarizes the transport parameters of relevant DHICA oligomers. The doubly oxidized dodecamer $\mathbf{Q_{2,11}}$ was used to model the hole trap state discussed in the main text.

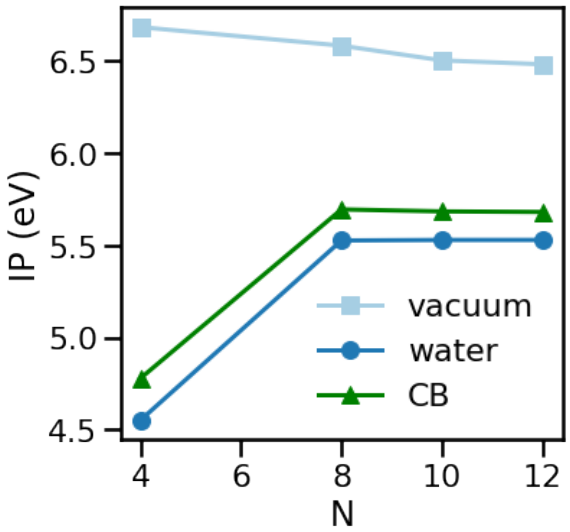

Figure S6. Ionization potential (IP) dependence on oligomer length for oxidized octamers, calculated in vacuum and with the SMD implicit solvation scheme.

Table S3. Ionization potentials, electron affinities and reorganization energies.

Structure	**IP**	**EA**	**λ^+**
Octamer	-	0.734	-
Octamer < >	5.87	-	0.514
Octamer $\mathbf{Q_7}$	6.58	3.58	0.686
Octamer $\mathbf{Q_8}$	-	3.07	-
Dodecamer < >	5.74	-	0.517
Dodecamer $\mathbf{Q_{11}}$	6.58	-	-
Dodecamer $\mathbf{Q_{2,11}}$	6.35	-	0.801